

---

---

# <sup>18</sup>F-FET PET Imaging in Differentiating Glioma Progression from Treatment-Related Changes: A Single-Center Experience

Gabriele D. Maurer<sup>1-3</sup>, Daniel P. Brucker<sup>2,3</sup>, Gabriele Stoffels<sup>4</sup>, Katharina Filipi<sup>3,5,6</sup>, Christian P. Filss<sup>4,7</sup>, Felix M. Mottaghy<sup>7-9</sup>, Norbert Galldiks<sup>\*4,9,10</sup>, Joachim P. Steinbach<sup>\*1-3</sup>, Elke Hattingen<sup>\*11</sup>, and Karl-Josef Langen<sup>\*4,7,9</sup>

<sup>1</sup>Dr. Senckenberg Institute of Neurooncology, Goethe University Hospital, Frankfurt am Main, Germany; <sup>2</sup>University Cancer Center Frankfurt, Goethe University Hospital, Frankfurt am Main, Germany; <sup>3</sup>German Cancer Consortium (DKTK), Partner Site Frankfurt/Mainz, Heidelberg, Germany; <sup>4</sup>Institute of Neuroscience and Medicine (INM-3 and INM-4), Research Center Juelich, Juelich, Germany; <sup>5</sup>German Cancer Research Center (DKFZ), Heidelberg, Germany; <sup>6</sup>Institute of Neurology (Edinger Institute), Goethe University Hospital, Frankfurt am Main, Germany; <sup>7</sup>Department of Nuclear Medicine, RWTH University Hospital, Aachen, Germany; <sup>8</sup>Department of Radiology and Nuclear Medicine, Maastricht University Medical Center, Maastricht, The Netherlands; <sup>9</sup>Center of Integrated Oncology, Universities of Aachen, Bonn, Cologne, and Duesseldorf, Germany; <sup>10</sup>Department of Neurology, University Hospital Cologne, Cologne, Germany; and <sup>11</sup>Institute of Neuroradiology, Goethe University Hospital, Frankfurt am Main, Germany

---

In glioma patients, differentiation between tumor progression (TP) and treatment-related changes (TRCs) remains challenging. Difficulties in classifying imaging alterations may result in a delay or an unnecessary discontinuation of treatment. PET using O-(2-<sup>18</sup>F-fluoroethyl)-L-tyrosine (<sup>18</sup>F-FET) has been shown to be a useful tool for detecting TP and TRCs. **Methods:** We retrospectively evaluated 127 consecutive patients with World Health Organization grade II–IV glioma who underwent <sup>18</sup>F-FET PET imaging to distinguish between TP and TRCs. <sup>18</sup>F-FET PET findings were verified by neuropathology (40 patients) or clinicoradiologic follow-up (87 patients). Maximum tumor-to-brain ratios (TBR<sub>max</sub>) of <sup>18</sup>F-FET uptake and the slope of the time–activity curves (20–50 min after injection) were determined. The diagnostic accuracy of <sup>18</sup>F-FET PET parameters was evaluated by receiver-operating-characteristic analysis and  $\chi^2$  testing. The prognostic value of <sup>18</sup>F-FET PET was estimated using the Kaplan–Meier method. **Results:** TP was diagnosed in 94 patients (74%) and TRCs in 33 (26%). For differentiating TP from TRCs, receiver-operating-characteristic analysis yielded an optimal <sup>18</sup>F-FET TBR<sub>max</sub> cutoff of 1.95 (sensitivity, 70%; specificity, 71%; accuracy, 70%; area under the curve, 0.75 ± 0.05). The highest accuracy was achieved by a combination of TBR<sub>max</sub> and slope (sensitivity, 86%; specificity, 67%; accuracy, 81%). However, accuracy was poorer when tumors harbored isocitrate dehydrogenase (*IDH*) mutations (91% in *IDH*-wild-type tumors, 67% in *IDH*-mutant tumors,  $P < 0.001$ ). <sup>18</sup>F-FET PET results correlated with overall survival ( $P < 0.001$ ). **Conclusion:** In our neurooncology department, the diagnostic performance of <sup>18</sup>F-FET PET was convincing but slightly inferior to that of previous reports.

**Key Words:** <sup>18</sup>F-FET PET; glioma; tumor progression; pseudoprogression; treatment-related changes

**J Nucl Med 2020; 61:505–511**

DOI: 10.2967/jnumed.119.234757

---

**G**liomas account for approximately 26% of primary central nervous system tumors and, among these, for 81% of malignant neoplasms (1). Clinical decision making considerably depends on glioma classification, based on histologic and molecular parameters (2), and imaging features. Despite some advances in surgical management and treatment regimens, grade II–IV gliomas remain incurable diseases with a decreased life expectancy.

The effectiveness of a treatment strategy is evaluated using the Response Assessment in Neuro-Oncology (RANO) criteria (3–5), which integrate MRI parameters, corticosteroid dosage, and the patient's performance status. Nevertheless, differentiation between treatment-related changes (TRCs) and actual tumor progression (TP) continues to be a crucial issue (6). A frequent problem is the so-called pseudoprogression, which describes the phenomenon that, in the absence of actual tumor growth, the diameter of contrast-enhancing areas enlarges by more than 25% or new lesions occur during or after therapy, mimicking tumor progression within the first 3 mo after chemoradiation completion with subsequent improvement of MRI findings (7–9). Within the spectrum of TRCs, radionecrosis is also of clinical relevance. Radionecrosis denotes an irradiation-related injury to brain tissue that may occur several months or even years after radiotherapy has been completed (10,11).

Because TRCs may raise concerns about whether therapy should be initiated, continued, or changed, various imaging techniques, including MRI methods and PET, are under consideration to better distinguish TRCs from TP (12–14). In this context, PET using O-(2-<sup>18</sup>F-fluoroethyl)-L-tyrosine (<sup>18</sup>F-FET) has been shown to provide additional information (15–18) and has recently been recommended by the RANO group (19). Some studies have already investigated the performance of <sup>18</sup>F-FET PET in glioma. However, they either

---

Received Aug. 5, 2019; revision accepted Sep. 6, 2019.  
For correspondence or reprints contact: Gabriele D. Maurer, Dr. Senckenberg Institute of Neurooncology, Goethe University Hospital, Schleusenweg 2-16, 60528 Frankfurt am Main, Germany.  
E-mail: gabriele.maurer@kgu.de  
\*Contributed equally to this work.  
Published online Sep. 13, 2019.  
COPYRIGHT © 2020 by the Society of Nuclear Medicine and Molecular Imaging.

were based on smaller patient populations (16,17,20–25) or included only a minor fraction of patients with TRCs (15).

In our neurooncology department, we recommended <sup>18</sup>F-FET PET imaging when conventional MRI and clinical assessment left some ambiguity as to whether TP or sequelae of therapy prevailed. We here outline our experience and focus on the diagnostic performance of additional <sup>18</sup>F-FET PET scans in clinical routine.

## MATERIALS AND METHODS

### Subjects

This retrospective study included 127 patients who were treated at the neurooncology department of the Goethe University Hospital in Frankfurt and, on the recommendation of the multidisciplinary tumor board and to distinguish between TP and TRCs, were referred to the nuclear medicine department of the University Hospital in Aachen at the Forschungszentrum Jülich for <sup>18</sup>F-FET PET imaging between March 2016 and January 2019. The analysis was approved by the scientific board of the University Cancer Center Frankfurt and by the local ethics committee (project SNO-8-2018). All patients had undergone standard MRI before, were able to understand the reason for additional <sup>18</sup>F-FET PET imaging, and gave written informed consent to the examination. One hundred twenty-five patients had previously been diagnosed with World Health Organization (WHO) grade II–IV glioma, and 2 patients had been treated for suspected glioma without prior biopsy.

### <sup>18</sup>F-FET PET Imaging

The amino acid <sup>18</sup>F-FET was synthesized and applied as described previously (26). All patients underwent a dynamic PET scan from 0 to 50 min after injection of 3 MBq of <sup>18</sup>F-FET per kilogram of body weight. The interval between MRI and <sup>18</sup>F-FET PET ranged from 0 to 77 d (median, 12 d). One hundred two patients were measured on a

stand-alone PET scanner (ECAT EXACT HR+; Siemens Healthcare) in 3-dimensional mode, and 25 patients were measured on a high-resolution 3-T hybrid PET/MR scanner (BrainPET; Siemens Healthcare) (22,25). Because of the reconstruction parameters and postprocessing steps, the different scanner types did not affect the quantitative <sup>18</sup>F-FET PET parameters (27).

### Postprocessing of <sup>18</sup>F-FET PET Images

Mean tumoral <sup>18</sup>F-FET uptake was determined by a 2-dimensional automatic contouring process using a tumor-to-brain ratio of at least 1.6 as described previously (22,25). For maximal amino acid uptake, a circular region of interest with a diameter of 1.6 cm was centered on maximal tumor uptake (15), to exclude an influence of different scanner resolutions. Mean and maximum tumor-to-brain ratio (TBR<sub>mean</sub> and TBR<sub>max</sub>) were calculated by dividing the SUV<sub>mean</sub> and SUV<sub>max</sub> of the tumor region of interest by the SUV<sub>mean</sub> of a larger crescent-shaped volume of interest placed in the semioval center of the contralateral unaffected hemisphere including white and gray matter (28,29).

Furthermore, time–activity curves for <sup>18</sup>F-FET uptake in the tumor were obtained by application of a spheric volume of interest with a diameter of 1.6 cm to the entire dynamic dataset. Time-to-peak values (minutes from the beginning of the dynamic acquisition up to the SUV<sub>max</sub> of the lesion) were derived from time–activity curves, and the slope of the time–activity curve in the late phase of <sup>18</sup>F-FET uptake was calculated by fitting a linear regression line to the late phase of the curve (20–50 min after injection). The slope was expressed as change in SUV per hour.

### Diagnosis of Tumor Progression and TRCs

TP or TRCs were confirmed by histopathologic examination after resection or biopsy or by clinicoradiologic follow-up. For WHO grade II gliomas, both the clinical and the radiologic situation had to be stable or improved for at least 12 mo without administration of

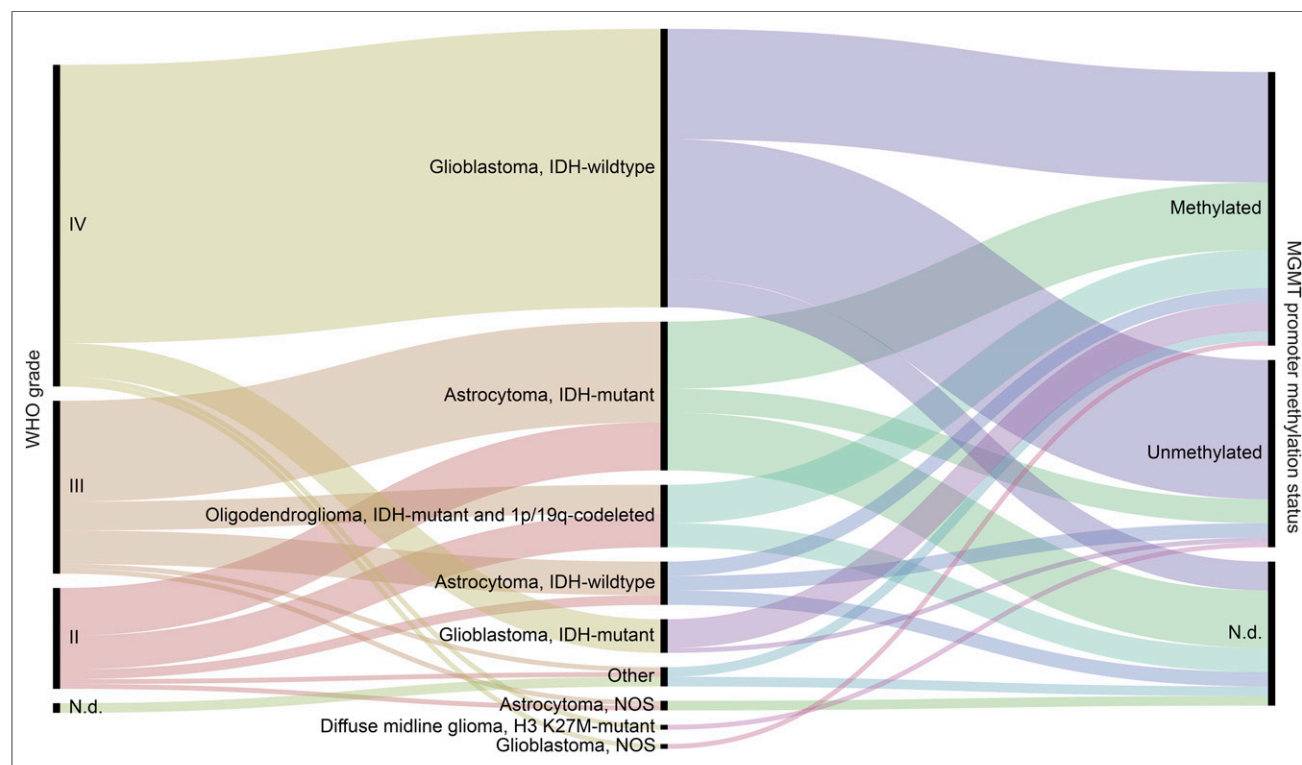


**FIGURE 1.** WHO grade, diagnosis according to WHO 2016 classification of brain tumors (2), and *MGMT* promoter methylation status of tumors that were later examined with <sup>18</sup>F-FET PET; N.d. = not determined or inconclusive.

**TABLE 1**  
Patient and Tumor Characteristics, Part 1

Characteristic	Data	%
<b>Sex (n)</b>		
Male	83	65
Female	44	35
<b>Age when <sup>18</sup>F-FET PET imaging was performed (y)</b>		
Mean ± SD	50 ± 12	
Range	20–78	
<b>KPS when <sup>18</sup>F-FET PET imaging was performed (n)</b>		
100%	49	39
90%	46	36
80%	19	15
70%	11	9
60%	2	2
<b>Interval between last therapy and <sup>18</sup>F-FET PET scan (d)</b>		
Median	103	
Range	0–3,540	
<b>Therapy before <sup>18</sup>F-FET PET imaging (n)</b>		
Radiotherapy	114	90
Chemotherapy		
Temozolomide	106	83
Lomustine-containing regimen	29	23
Bevacizumab	9	7
Tumor treating fields	9	7
Reresection	21	17
Reirradiation	19	15
Nivolumab	7	6
Other*	6	5

\*This section included 3 patients treated with nivolumab or placebo in context of clinical trial, 1 patient treated with sitimogene ceradenovec/ganciclovir, 1 patient treated with brachytherapy using <sup>125</sup>I seeds, and 1 patient treated with irinotecan.

KPS = Karnofsky performance status.

another therapy to exclude TP (16). For WHO grade III–IV gliomas, the classification of TRCs required at least 6 mo of a stable or improved clinical and radiologic condition (17), as well as no change in tumor treatment. TP was considered present when lesions continued to increase in size on at least 2 subsequent MRI scans according to the RANO criteria, paralleled by a deterioration in performance status, or when a patient died of glioma, whichever occurred first. Thus, the classification criteria in our study were similar to those of previous investigations (25,30,31) or were more stringent (20).

### Neuropathology

Tissue obtained from resection or biopsy was fixed in 4% paraformaldehyde and paraffin-embedded. Sections 3 μm thick were cut on an SM 2000R microtome (Leica Biosystems), mounted on microscope slides (SuperFrost Plus; Thermo Scientific), and subjected to

hematoxylin–eosin staining. Immunohistochemistry against the isocitrate dehydrogenase (*IDH*) mutation-specific antibody IDH1\_R132H (mouse monoclonal, clone DIA-H09, concentration 1:50; Dianova) was performed according to standardized protocols using a Leica BOND-III stainer. A tumor was considered to be progressive when it was seen to be solid in histologic workup; the occurrence of single—for

**TABLE 2**  
Patient and Tumor Characteristics, Part 2

Characteristic	Data	%
<b>Diagnosis (n)</b>		
Glioblastoma, <i>IDH</i> -wild-type, WHO IV	59	46
Glioblastoma, <i>IDH</i> -mutant, WHO IV	7	6
Glioblastoma, not otherwise specified, WHO IV	1	0.8
Astrocytoma, <i>IDH</i> -wild-type		
WHO II	2	2
WHO III	7	6
Astrocytoma, <i>IDH</i> -mutant		
WHO II	10	8
WHO III	21	17
Astrocytoma, not otherwise specified		
WHO II	1	0.8
WHO III	1	0.8
Oligodendroglioma, <i>IDH</i> -mutant and 1p/19q-codeleted		
WHO II	7	6
WHO III	6	5
Diffuse midline glioma, H3 K27 M-mutant, WHO IV	1	0.8
Other*		
WHO II	1	0.8
WHO III	1	0.8
ND	2	2
<b>MGMT promoter methylation status (n)</b>		
Methylated	57	45
Unmethylated	40	31
ND	30	24
<b>Extent of resection at initial diagnosis (n)</b>		
Gross total resection	67	53
Subtotal resection	8	6
Partial resection	20	16
Biopsy	30	24
None	2	2

\*This section included 1 diffuse glioma, *IDH*-wild-type, nuclear ATRX retained, *MGMT* promoter methylated; 1 anaplastic glioma, *IDH*-mutant, nuclear ATRX retained, *MGMT* promoter methylated; 1 suspected diffuse pontine glioma (treated without prior biopsy); and 1 suspected diffuse medulla oblongata glioma (treated without prior biopsy).

ND = not determined or inconclusive.

example, IDH1\_R132H-positive—tumor cells was not sufficient for diagnosis of TP. TRCs, on the other hand, were characterized as a lack of solid tumor or the presence of radiogenic necrosis, hyalinized vessel walls, or resorptive changes.

### Statistical Analysis

Data were analyzed using Excel (Microsoft), SPSS Statistics (version 25; IBM), and SigmaPlot (version 11.0; Systat Software). Continuously scaled variables were compared by the Mann–Whitney rank sum test or the Student *t* test for independent samples, and categorical variables were compared by the Pearson  $\chi^2$  test or the Fisher exact test. Survival was calculated from the date of  $^{18}\text{F}$ -FET PET imaging to the date of death or the last follow-up visit, and survival distributions were analyzed using the log-rank test. Univariate and multivariate Cox regression models were applied to identify prognostic parameters. A *P* value of less than 0.05 was considered significant. The diagnostic performance of the  $^{18}\text{F}$ -FET PET parameters  $\text{TBR}_{\text{max}}$ ,  $\text{TBR}_{\text{mean}}$ , time-to-peak value, and slope for differentiation of TP from TRCs was assessed by receiver-operating-characteristic curve analyses using the neuropathologic results or the clinicoradiologic follow-up as a reference. The decision cutoff was considered optimal when the

product of paired values for sensitivity and specificity reached its maximum. Visualization was performed using Excel, Illustrator (Adobe), and RAWGraphs (<http://app.rawgraphs.io/>) (32).

### RESULTS

Patient and tumor characteristics are depicted in Figure 1, Tables 1 and 2, and Supplemental Table 1 (supplemental materials are available at <http://jnm.snmjournals.org>).

Repeated resection was performed for 36 patients and biopsy for 4 patients. The median time from  $^{18}\text{F}$ -FET PET to surgery was 21.5 d (range, 10–215 d) and was longer when  $^{18}\text{F}$ -FET PET indicated TRCs (6 patients; median, 90 d; range, 12–215 d) than when  $^{18}\text{F}$ -FET PET suggested TP (34 patients; median, 19 d; range, 10–119 d). Eighty-seven patients were evaluated on the basis of clinicoradiologic follow-up. Until June 2019, 57 of the 127 patients succumbed to their disease (median time from  $^{18}\text{F}$ -FET PET to death, 208 d; range, 24–950 d), and 70 continued follow-up (median time from  $^{18}\text{F}$ -FET PET to last follow-up visit, 484 d; range, 128–1,050 d).

Receiver-operating-characteristic analysis yielded a  $\text{TBR}_{\text{max}}$  of

1.95 as an optimal cutoff to identify TP (sensitivity, 70%; specificity, 71%; area under the curve,  $0.76 \pm 0.05$ ;  $P < 0.001$ ).

The cutoff for the  $\text{TBR}_{\text{mean}}$  to detect TP was also 1.95 (sensitivity, 56%; specificity, 79%; accuracy, 62%; area under the curve,  $0.75 \pm 0.05$ ;  $P < 0.001$ ). The time-to-peak value did not allow discrimination between TP and TRCs (area under the curve, 0.58;  $P = 0.15$ ). For slope, the optimal cutoff to show TP was less than 0.2 SUV/h (sensitivity, 54%; specificity, 86%; accuracy, 63%; area under the curve,  $0.69 \pm 0.05$ ;  $P < 0.001$ ). The combined analysis of a  $\text{TBR}_{\text{max}}$  greater than 1.95 or a slope less than 0.2 SUV/h revealed TP best, with a sensitivity of 86%, a specificity of 67%, and an accuracy of 81% ( $P < 0.001$ ). In individual cases (6 patients), further criteria such as a focal hotspot that was underestimated by the region-of-interest analysis, or an increasing  $^{18}\text{F}$ -FET uptake compared with a previous  $^{18}\text{F}$ -FET PET examination, were also considered indicators of TP (Supplemental Table 1). Supplemental Tables 2 and 3 summarize the diagnoses based on  $^{18}\text{F}$ -FET PET findings. Figure 2 depicts examples of false-positive and -negative  $^{18}\text{F}$ -FET PET ratings.

Overall survival was longer when, finally, TRCs were diagnosed (Fig. 3A), as well as when  $^{18}\text{F}$ -FET PET results indicated TRCs (Fig. 3B). The results of univariate and multivariate survival analyses are given in Table 3. In multivariate evaluation, we fitted a stepwise-backward exclusion model including the  $^{18}\text{F}$ -FET PET rating, the tumor grade, the *IDH* status, the O6-methylguanine-DNA methyltransferase (*MGMT*) promoter methylation status, the patient's age, and the patient's Karnofsky performance status. The  $^{18}\text{F}$ -FET PET rating, the WHO grade, the

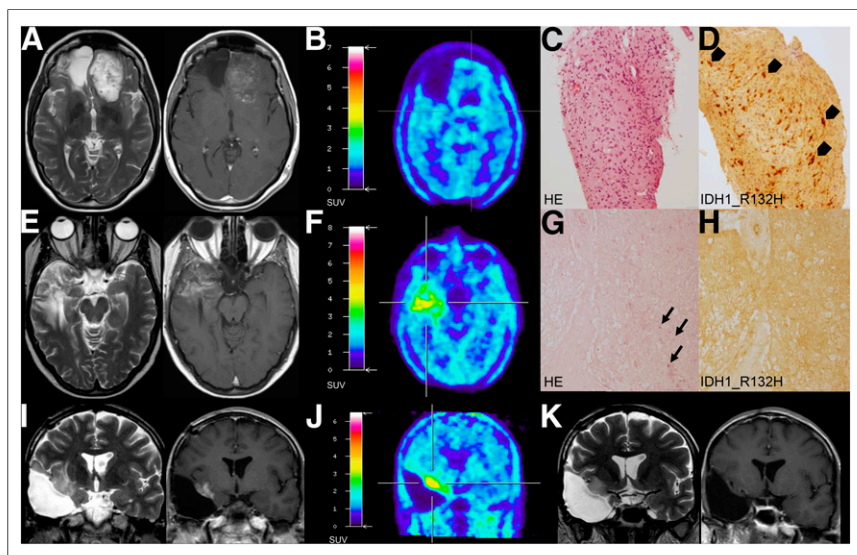


**FIGURE 2.** Examples of false-negative and -positive  $^{18}\text{F}$ -FET PET ratings. (A–D) A 45-y-old-patient had been diagnosed with *IDH*-mutant, *MGMT* promoter methylated glioblastoma in November 2010. After gross total resection, radiotherapy, and irinotecan chemotherapy, she received bevacizumab every other week. In January 2017, follow-up MRI indicated disease progression (RANO criteria). However, in February 2017,  $^{18}\text{F}$ -FET PET imaging was not suggestive of tumor, and so patient continued follow-up. Subsequent MRI revealed enlargement of both contrast-enhancing and non-contrast-enhancing lesions (tumor progression, RANO criteria), but  $^{18}\text{F}$ -FET PET remained negative. In November 2017, biopsy revealed tumor progression. Shown are axial MRI, October 2017, T2 image (A, left) and contrast-enhanced T1 image (A, right);  $^{18}\text{F}$ -FET PET, November 2017 (B); and histology (hematoxylin-eosin [HE]) (C) and immunohistochemistry (IDH1\_R132H, arrowheads point to IDH1\_R132H-positive tumor cells) (D) of biopsy samples, November 2017. (E–H) A 39-y-old patient had undergone subtotal resection of IDH1\_R132H-mutant and 1p/19q-codeleted oligodendroglioma in August 2010, temozolomide chemotherapy until January 2011, proton therapy in May and June 2015, and lomustine chemotherapy from July to December 2015. In July 2017, putative recurrent tumor was resected. Neuropathology showed sequelae of radiation but no tumor. Shown are axial MRI, May 2017, T2 image (E, left) and contrast-enhanced T1 image (E, right);  $^{18}\text{F}$ -FET PET indicating tumor progression, June 2017 (F); and necrosis and calcification (arrows, HE) (G) without IDH1\_R132H-positive tumor cells (H) in resected samples, July 2017. (I–K) *IDH*-mutant, *MGMT* promoter methylated glioblastoma of 38-y-old patient had been treated by partial resection in April 2016, radiotherapy, and temozolomide chemotherapy from April to June 2016. Against our advice, patient decided not to continue tumor-specific therapy. However, imaging alterations regressed spontaneously. Shown are coronal MRI, February 2017, T2 image (I, left) and contrast-enhanced T1 image (I, right);  $^{18}\text{F}$ -FET PET indicating tumor progression, April 2017 (J); and follow-up MRI, February 2018, T2 image (K, left) and contrast-enhanced T1 image (K, right).

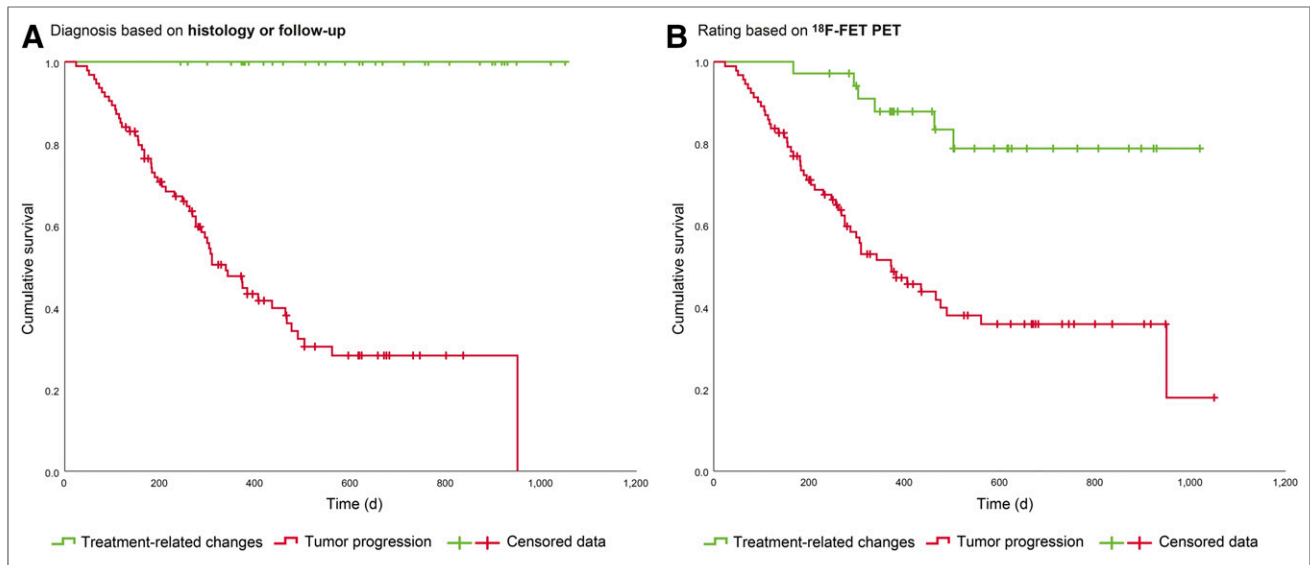


**FIGURE 3.** Overall survival of all 127 patients. (A) Overall survival after  $^{18}\text{F}$ -FET PET imaging, depending on whether TP or TRCs were present, as assessed by histology or follow-up ( $P$  [log-rank] < 0.001). (B) Overall survival after  $^{18}\text{F}$ -FET PET imaging, depending on  $^{18}\text{F}$ -FET PET results ( $P$  [log-rank] < 0.001).

*IDH* status, and the Karnofsky performance status remained independent prognostic factors.

Looking at the tumor characteristics, we noticed that the accuracy of  $^{18}\text{F}$ -FET PET was higher in *IDH*-wild-type gliomas than in *IDH*-mutant ones ( $P < 0.001$ ). The diagnosis based on  $^{18}\text{F}$ -FET PET turned out to be incorrect in 33% of the *IDH*-mutant tumors (11 true-negative, 23 true-positive, 8 false-positive, and 9 false-negative results) but in only 9% of the *IDH*-wild-type tumors

(8 true-negative, 56 true-positive, 3 false-positive, and 3 false-negative results). *MGMT* promoter methylation did not significantly affect the diagnostic performance of  $^{18}\text{F}$ -FET PET.

## DISCUSSION

Diagnosis and treatment of brain tumors are strongly linked to imaging techniques, especially MRI techniques, because histologic

**TABLE 3**  
Univariate and Multivariate Analyses of Overall Survival

Survival analysis	Patients (n)	HR	95% CI	P
<b>Univariate</b>				
Diagnosis based on $^{18}\text{F}$ -FET PET	127	4.997	2.139–11.675	<0.001
<i>IDH</i> status				
<i>IDH</i> -wild-type	70	1.000		
<i>IDH</i> -mutant	51	0.181	0.091–0.363	<0.001
<i>MGMT</i> promoter methylation status				
Unmethylated	40	1.000		
Methylated	57	0.493	0.278–0.877	0.016
WHO grade	125	3.859	2.230–6.678	<0.001
Age (y)	127	1.043	1.020–1.066	<0.001
KPS (%)	127	0.965	0.940–0.990	0.007
Number of glioma recurrences before $^{18}\text{F}$ -FET PET scan	127	1.051	0.792–1.395	NS
Interval between last therapy and $^{18}\text{F}$ -FET PET scan (d)	124	0.997	0.996–0.999	0.001
<b>Multivariate</b>				
Diagnosis based on $^{18}\text{F}$ -FET PET		3.424	1.446–8.109	0.005
WHO grade		2.143	1.212–3.792	0.009
<i>IDH</i> status		0.412	0.210–0.808	0.010
KPS (%)		0.975	0.950–1.001	0.057

HR = hazard ratio; CI = confidence interval; KPS = Karnofsky performance status; NS = not statistically significant.

confirmation often cannot be realized easily and without substantial risk.  $^{18}\text{F}$ -FET PET is not a standard method for the assessment of TP in glioma but may be more accurate than conventional MRI (14,25) and helpful in complex or challenging cases (19). In our department, we consider this method in particular when MRI yields inconclusive results. The present report outlines our experience with  $^{18}\text{F}$ -FET PET in differentiating TP from TRCs in WHO grade II–IV gliomas.  $^{18}\text{F}$ -FET PET based on  $\text{TBR}_{\text{max}}$  achieved an accuracy of 70%, which could be increased to 81% by combination with kinetic parameters. However, these values are in the low range compared with previous studies.

Retrospectively analyzing 132 scans of 124 WHO grade II–IV glioma patients, Galldiks et al. described an accuracy of 93% for  $^{18}\text{F}$ -FET PET to diagnose TP (15), but the number of patients with TRCs in that study, namely 8%, was quite small and might have influenced the results. Looking at 45 patients suspected of having TP, Rachinger et al. found a sensitivity of 100% and a specificity of 93% for  $^{18}\text{F}$ -FET PET imaging (21). Kebir et al. noted a sensitivity of 84%, a specificity of 86%, and an accuracy of 85% for  $^{18}\text{F}$ -FET PET to differentiate between TP and pseudoprogression in a series of 26 patients (20). In a study on 36 glioblastoma patients conducted by Mihovilovic et al., static  $^{18}\text{F}$ -FET PET discriminated between TP and TRCs with a sensitivity of 89%, a specificity of 75%, and an accuracy of 86% (31). Analyzing the  $^{18}\text{F}$ -FET PET scans of 48 high-grade glioma patients, Werner et al. reported a prevalence of 21% for TRCs and a 93% diagnostic accuracy for static and dynamic  $^{18}\text{F}$ -FET PET parameters (25). In our study, the percentage of patients with TRCs was similar to that in other studies (20,25,31), but the diagnostic performance of  $^{18}\text{F}$ -FET PET imaging was slightly inferior (20,23,31).

One must consider that all patients in this study were treated in a single neurooncology department with procedures that were based on weekly discussions in multidisciplinary tumor conferences. Therefore, the decision-making process should have been consistent but carried several biases. First,  $^{18}\text{F}$ -FET PET imaging was not part of the routine workup of patients with suspected TP. Many patients initially underwent MR perfusion and spectroscopy, and often  $^{18}\text{F}$ -FET PET was recommended merely in cases of ambiguity. Therefore, the patient group might represent a selection of particularly difficult cases, which in turn could lead to an underestimation of the accuracy of  $^{18}\text{F}$ -FET PET. Second, imaging was considered appropriate only if it resulted in therapeutic consequences. That is why patients with a poor performance status or without further treatment options were not assigned to receive  $^{18}\text{F}$ -FET PET imaging. Third, a higher rate of histologic confirmation after  $^{18}\text{F}$ -FET PET would have been desirable, but resection or biopsy was not routinely performed when the imaging aspect was ambiguous. Invasive interventions were suggested only if all evidence pointed toward TP. However, the sole inclusion of patients with histologic confirmation would lead to a different bias, especially to the exclusion of true-negative results. Despite these limitations, this study probably reflects the current situation in many centers, as  $^{18}\text{F}$ -FET PET is not generally available as a routine tool and can be used only in selected indications.

An interesting new observation in our study was that the accuracy of  $^{18}\text{F}$ -FET PET in differentiating TP from TRCs was significantly higher in *IDH*-wild-type tumors than in *IDH*-mutant ones. This knowledge could be helpful when considering  $^{18}\text{F}$ -FET PET as an additional diagnostic tool. Possibly, previous studies did not reveal this aspect because of a lack of molecular markers, smaller collectives, or a minor fraction of patients with TRCs. It is certainly worth further investigation and should be verified in a

larger number of patients. In view of the current literature, we cannot clearly explain this finding, especially false-positive  $^{18}\text{F}$ -FET PET results. Compared with *IDH*-wild-type tumors, *IDH*-mutant gliomas are considered less immunologically active (33), and the presence of mutant *IDH* has been shown to impair complement activation, infiltration of CD45-positive immune cells, T-cell migration, proliferation, and activity (34). Because inflammation may contribute to the  $^{18}\text{F}$ -FET PET signal under certain circumstances (14), immunosuppression might mask tumor growth and lead to false-negative results.

## CONCLUSION

$^{18}\text{F}$ -FET PET complemented our current diagnostic portfolio, drove decision making, and independently predicted survival. The interpretation of results should consider the tumor's *IDH* status because, in our study, the accuracy of  $^{18}\text{F}$ -FET PET was higher in *IDH*-wild-type gliomas.

## DISCLOSURE

The Dr. Senckenberg Institute of Neurooncology is supported by the Dr. Senckenberg foundation (grant 2014/SIN-02). Joachim Steinbach has received a grant from Merck, as well as honoraria for lectures, travel, or advisory board participation from Roche, Medac, Bristol-Myers Squibb, and Abbvie. No other potential conflict of interest relevant to this article was reported.

## ACKNOWLEDGMENTS

We thank all the patients and their families for participating in this study; the nurses and assistants at the Dr. Senckenberg Institute of Neurooncology for supporting the outpatient procedures; Erika Wabbals, Silke Grafmueller, and Sascha Rehbein for technical assistance in radiosynthesis of  $^{18}\text{F}$ -FET; and Silke Frensch, Suzanne Schaden, Kornelia Frey, and Trude Plum for technical assistance in performing the PET measurements at the Forschungszentrum Jülich.

## KEY POINTS

**QUESTION:** How well can  $^{18}\text{F}$ -FET PET help to distinguish between TP and TRCs?

**PERTINENT FINDINGS:** In this retrospective analysis of patients with WHO grade II–IV glioma treated at our neurooncology department, the diagnostic accuracy of  $^{18}\text{F}$ -FET PET was slightly inferior to that of previous reports and was higher in *IDH*-wild-type than in *IDH*-mutant tumors. The  $^{18}\text{F}$ -FET PET rating was prognostic of survival.

**IMPLICATIONS FOR PATIENT CARE:**  $^{18}\text{F}$ -FET PET provided valuable information. Our observation that its accuracy depended on the *IDH* status might be crucial for decision making.

## REFERENCES

- Ostrom QT, Gittleman H, Truitt G, Boscia A, Kruchko C, Barnholtz-Sloan JS. CBTRUS statistical report: primary brain and other central nervous system tumors diagnosed in the United States in 2011–2015. *Neuro-oncol.* 2018;20:iv1–iv86.
- Louis DN, Perry A, Reifenberger G, et al. The 2016 World Health Organization classification of tumors of the central nervous system: a summary. *Acta Neuropathol (Berl).* 2016;131:803–820.

3. Wen PY, Macdonald DR, Reardon DA, et al. Updated response assessment criteria for high-grade gliomas: response assessment in neuro-oncology working group. *J Clin Oncol*. 2010;28:1963–1972.
4. van den Bent MJ, Wefel J, Schiff D, et al. Response assessment in neuro-oncology (a report of the RANO group): assessment of outcome in trials of diffuse low-grade gliomas. *Lancet Oncol*. 2011;12:583–593.
5. Ellingson BM, Wen PY, Cloughesy TF. Modified criteria for radiographic response assessment in glioblastoma clinical trials. *Neurotherapeutics*. 2017;14:307–320.
6. Hygino da Cruz LC, Rodriguez I, Domingues RC, Gasparetto EL, Sorensen AG. Pseudoprogression and pseudoresponse: imaging challenges in the assessment of posttreatment glioma. *AJNR Am J Neuroradiol*. 2011;32:1978–1985.
7. Thust SC, van den Bent MJ, Smits M. Pseudoprogression of brain tumors. *J Magn Reson Imaging*. 2018;48:571–589.
8. Brandsma D, Stalpers L, Taal W, Sminia P, van den Bent MJ. Clinical features, mechanisms, and management of pseudoprogression in malignant gliomas. *Lancet Oncol*. 2008;9:453–461.
9. Hoffman WF, Levin VA, Wilson CB. Evaluation of malignant glioma patients during the postirradiation period. *J Neurosurg*. 1979;50:624–628.
10. Siu A, Wind JJ, Iorgulescu JB, Chan TA, Yamada Y, Sherman JH. Radiation necrosis following treatment of high grade glioma: a review of the literature and current understanding. *Acta Neurochir (Wien)*. 2012;154:191–201.
11. Delgado-López PD, Riñones-Mena E, Corrales-García EM. Treatment-related changes in glioblastoma: a review on the controversies in response assessment criteria and the concepts of true progression, pseudoprogression, pseudoresponse and radionecrosis. *Clin Transl Oncol*. 2018;20:939–953.
12. van Dijken BRJ, van Laar PJ, Holtman GA, van der Hoorn A. Diagnostic accuracy of magnetic resonance imaging techniques for treatment response evaluation in patients with high-grade glioma, a systematic review and meta-analysis. *Eur Radiol*. 2017;27:4129–4144.
13. Prager AJ, Martinez N, Beal K, Omuro A, Zhang Z, Young RJ. Diffusion and perfusion MRI to differentiate treatment-related changes including pseudoprogression from recurrent tumors in high-grade gliomas with histopathologic evidence. *AJNR Am J Neuroradiol*. 2015;36:877–885.
14. Langen K-J, Galldiks N, Hattungen E, Shah NJ. Advances in neuro-oncology imaging. *Nat Rev Neurol*. 2017;13:279–289.
15. Galldiks N, Stoffels G, Filss C, et al. The use of dynamic O-(2-<sup>18</sup>F-fluoroethyl)-L-tyrosine PET in the diagnosis of patients with progressive and recurrent glioma. *Neuro-oncol*. 2015;17:1293–1300.
16. Pöpperl G, Götz C, Rachinger W, Gildehaus F-J, Tonn J-C, Tatsch K. Value of O-(2-[<sup>18</sup>F]fluoroethyl)-L-tyrosine PET for the diagnosis of recurrent glioma. *Eur J Nucl Med Mol Imaging*. 2004;31:1464–1470.
17. Mehrkens JH, Pöpperl G, Rachinger W, et al. The positive predictive value of O-(2-[<sup>18</sup>F]fluoroethyl)-L-tyrosine (FET) PET in the diagnosis of a glioma recurrence after multimodal treatment. *J Neurooncol*. 2008;88:27–35.
18. la Fougère C, Suchorska B, Bartenstein P, Kreth F-W, Tonn J-C. Molecular imaging of gliomas with PET: opportunities and limitations. *Neuro-oncol*. 2011;13:806–819.
19. Albert NL, Weller M, Suchorska B, et al. Response assessment in Neuro-Oncology Working Group and European Association for Neuro-Oncology recommendations for the clinical use of PET imaging in gliomas. *Neuro-oncol*. 2016;18:1199–1208.
20. Kebir S, Fimmers R, Galldiks N, et al. Late pseudoprogression in glioblastoma: diagnostic value of dynamic O-(2-[<sup>18</sup>F]fluoroethyl)-L-tyrosine PET. *Clin Cancer Res*. 2016;22:2190–2196.
21. Rachinger W, Goetz C, Pöpperl G, et al. Positron emission tomography with O-(2-[<sup>18</sup>F]fluoroethyl)-L-tyrosine versus magnetic resonance imaging in the diagnosis of recurrent gliomas. *Neurosurgery*. 2005;57:505–511.
22. Cecon G, Lazaridis L, Stoffels G, et al. Use of FET PET in glioblastoma patients undergoing neurooncological treatment including tumour-treating fields: initial experience. *Eur J Nucl Med Mol Imaging*. 2018;45:1626–1635.
23. Pyka T, Hiob D, Preibisch C, et al. Diagnosis of glioma recurrence using multiparametric dynamic <sup>18</sup>F-fluoroethyl-tyrosine PET-MRI. *Eur J Radiol*. 2018;103:32–37.
24. Jena A, Taneja S, Gambhir A, et al. Glioma recurrence versus radiation necrosis: single-session multiparametric approach using simultaneous O-(2-<sup>18</sup>F-fluoroethyl)-L-tyrosine PET/MRI. *Clin Nucl Med*. 2016;41:e228–e236.
25. Werner J-M, Stoffels G, Lichtenstein T, et al. Differentiation of treatment-related changes from tumour progression: a direct comparison between dynamic FET PET and ADC values obtained from DWI MRI. *Eur J Nucl Med Mol Imaging*. 2019;46:1889–1901.
26. Hamacher K, Coenen HH. Efficient routine production of the <sup>18</sup>F-labelled amino acid O-2-<sup>18</sup>F fluoroethyl-L-tyrosine. *Appl Radiat Isot*. 2002;57:853–856.
27. Lohmann P, Herzog H, Rota Kops E, et al. Dual-time-point O-(2-[<sup>18</sup>F]fluoroethyl)-L-tyrosine PET for grading of cerebral gliomas. *Eur Radiol*. 2015;25:3017–3024.
28. Unterrainer M, Vettermann F, Brendel M, et al. Towards standardization of <sup>18</sup>F-FET PET imaging: do we need a consistent method of background activity assessment? *EJNMMI Res*. 2017;7:48.
29. Law I, Albert NL, Arbizu J, et al. Joint EANM/EANO/RANO practice guidelines/SNMMI procedure standards for imaging of gliomas using PET with radio-labelled amino acids and [<sup>18</sup>F]FDG: version 1.0. *Eur J Nucl Med Mol Imaging*. 2019;46:540–557.
30. Young RJ, Gupta A, Shah AD, et al. Potential utility of conventional MRI signs in diagnosing pseudoprogression in glioblastoma. *Neurology*. 2011;76:1918–1924.
31. Mihovilovic MI, Kertels O, Hänscheid H, et al. O-(2-(<sup>18</sup>F)fluoroethyl)-L-tyrosine PET for the differentiation of tumour recurrence from late pseudoprogression in glioblastoma. *J Neurol Neurosurg Psychiatry*. 2019;90:238–239.
32. Mauri M, Elli T, Caviglia G, Ubaldi G, Azzi M. RAWGraphs: a visualisation platform to create open outputs. In: *Proceedings of the 12th Biannual Conference on Italian SIGCHI Chapter*. New York, NY: ACM Press; 2017:1–5.
33. Kaminska B, Czapski B, Guzik R, Król S, Gielniewski B. Consequences of IDH1/2 mutations in gliomas and an assessment of inhibitors targeting mutated IDH proteins. *Molecules*. 2019;24:968.
34. Lucca LE, Hafler DA. Resisting fatal attraction: a glioma oncometabolite prevents CD8+ T cell recruitment. *J Clin Invest*. 2017;127:1218–1220.